Journal of Marine Research, 63, 1127–1149, 2005

Origin and fate of a bloom of *Skeletonema costatum* during a winter upwelling/downwelling sequence in the Ría de Vigo (NW Spain)

by X. A. Álvarez–Salgado[1,2], **M. Nieto–Cid**[1], **S. Piedracoba**[3], **B. G. Crespo**[1], **J. Gago**[1], **S. Brea**[1], **I. G. Teixeira**[1], **F. G. Figueiras**[1], **J. L. Garrido**[1], **G. Rosón**[3], **C. G. Castro**[1] and **M. Gilcoto**[1]

ABSTRACT

The onset, development and decay of a winter bloom of the marine diatom *Skeletonema costatum* was monitored during a 10 d period in the coastal upwelling system of the Ría de Vigo (NW Spain). The succession of upwelling, relaxation and downwelling-favorable coastal winds with a frequency of 10–20 d is a common feature of the NW Iberian shelf. The onset of the bloom occurred during an upwelling-favorable ½ wk period under winter thermal inversion conditions. The subsequent ½ wk coastal wind relaxation period allowed development of the bloom (gross primary production reached 8 g C m^{-2} d^{-1}) utilizing nutrients upwelled during the previous period. Finally, downwelling during the following ½ wk period forced the decay of the bloom through a combination of cell sinking and downward advection.

1. Introduction

Understanding the origin, development, and fate of marine phytoplankton blooms is a key scientific issue, either from the viewpoint of the sustainable exploitation of marine living resources or the role played by the ocean in the regulation of Earth climate. The topic becomes specially relevant in ocean margins which represent less than 8% of the ocean surface area but comprise more than 25% of the ocean primary production (Wollast, 1998), up to 85% of the organic matter preserved in marine sediments (Middelburg *et al.,* 1993) and more than 90% of the fish catches (FAO Fisheries, 1997). Enhanced nutrient fluxes from continental runoff, the atmosphere and the adjacent open ocean (Walsh *et al.,* 1991), together with an efficient nutrient recycling based on a closed coupling between pelagic production and benthic regeneration (Wollast, 1993; 1998) are the reasons behind the high productivity of the coastal zone. All these biogeochemical processes are specially intensi-

1. CSIC, Instituto de Investigacións Mariñas, Eduardo Cabello 6, 36208–Vigo, Spain.
2. Corresponding author. ***email: xsalgado@iim.csic.es***
3. Universidad de Vigo, Grupo de Oceanografía Física, Unidad Asociada al CSIC, Facultad de Ciencias del Mar, Lagoas–Marcosende, Vigo, Spain.

fied in coastal upwelling regions because of the enhanced entry of nutrient salts from the adjacent ocean (Walsh *et al.,* 1991; Wollast, 1998).

The typical annual succession of microplankton species in coastal upwelling regions is characterized by diatom spring and dinoflagellate autumn blooms delimiting a summer period with significant contribution of heterotrophic components. The winter period is dominated by small flagellate species. However, considerable temporal and spatial variability affects this pattern in response to short-time-scale upwelling –relaxation cycles (e.g. Blasco *et al.,* 1980; Brink *et al.,* 1980; Figueiras *et al.,* 1994; Fermín *et al.,* 1996). Upwelling promotes diatom growth and relaxation favors other species better adapted to stratified conditions, such as dinoflagellates (Margalef, 1978). Consequently, upwelling causes sporadic breaks of succession, returning to earlier stages. The combination of (1) preceding phase of succession, (2) degree of water column stratification and (3) wind intensity determine the stage to which succession is reset (Estrada and Blasco, 1979). In this sense, coastal upwelling must be stronger during summer than in spring to cause a pioneer diatom bloom.

The annual cycle of chlorophyll concentration in NW Iberian shelf waters is a mixture of two main components (Nogueira *et al.,* 1997): (1) the classical pattern of temperate ecosystems, characterized by spring diatom and autumn dinoflagellate blooms separated by an unproductive winter (light–limited) period and a summer (nutrient–limited) period dominated by small flagellates in which heterotrophy is important (Figueiras and Rios, 1993); (2) short-time-scale (10-20 d) successions from diatom to flagellate populations in response to the conspicuous shelf wind-driven upwelling/relaxation cycles that succeed during the upwelling-favorable season, from March to October (Pazos *et al.,* 1995). It is remarkable that the spring diatom bloom occurs at the time of the transition from the downwelling- to the upwelling-favorable season, whereas the autumn dinoflagellates bloom at the time of the transition from the upwelling- to the downwelling-favorable season. The occurrence of upwelling or downwelling conditions during the development of these blooms has key implications for their origin, *in situ* growth *versus* accumulation, and fate, off-shelf export *versus in situ* respiration (Álvarez–Salgado *et al.,* 2003). In any case, the annual cycle of shelf wind stress explains less than 15% of the total variability of the wind patterns off NW Spain and more than 70% of that variability concentrates at periods of less than one month, the 10–20 d period of the upwelling/relaxation episodes during the upwelling-favorable season being especially relevant (Álvarez–Salgado *et al.,* 2002).

Although the short-time-scale hydrodynamic, chemical and biological response to the meteorological forcing of the NW Iberian shelf is relatively well characterized for the upwelling-favorable season, a clear lack of knowledge exists for the downwelling period. Short-time-scale wind-driven upwelling events have been described during the downwelling-favorable season (Nogueira *et al.,* 1997; Pardo *et al*., 2001; Álvarez *et al.,* 2003), but studies about the impact on phytoplankton ecology and biogeochemical cycles are restricted to the imprint in chlorophyll and nutrient concentrations (Nogueira *et al.,* 1997). The aim of this work is to determine the origin and fate of a winter phytoplankton bloom of

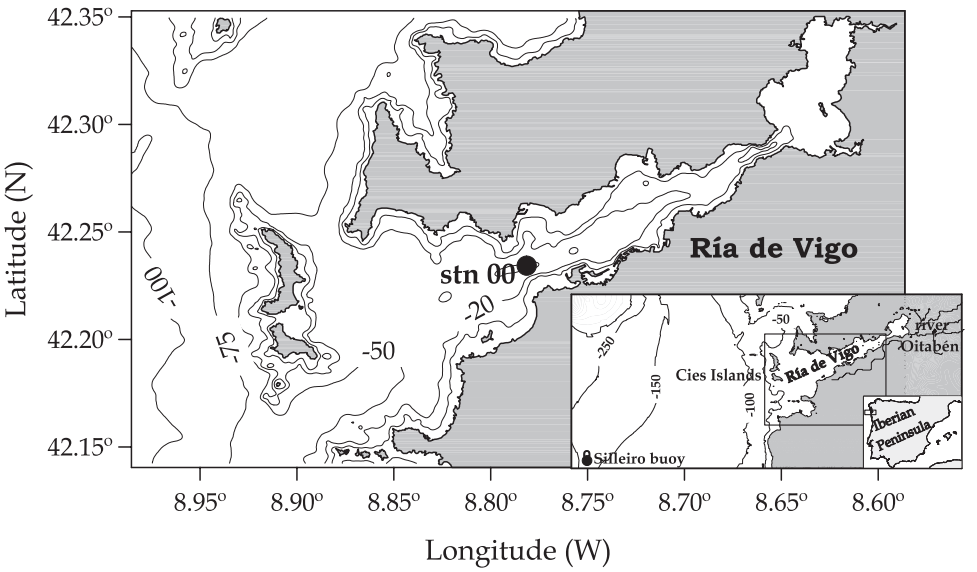

Figure 1. Chart of the Ría de Vigo (NW Spain), indicating the position of the sampling site (stn 00), where the ADCP current meter was moored, the Seawatch buoy of Puertos del Estado off Cape Silleiro (in 350 m water) and the meteorological station of the airport of Vigo. The -20, -50, -75 and -100 m isobaths are also included.

the pioneer diatom *S. costatum* that occurred in the Ría de Vigo (NW Spain) during a 10 d period in February 2002. Meteorological, hydrodynamic and hydrological (thermohaline, chemical and biological) field data and on-deck incubation experiments were combined to provide a realistic view of the onset, development and abrupt termination of a winter bloom.

2. Methods

a. Sampling strategy

The time series station (stn 00), placed in the middle segment of the Ría de Vigo (Fig. 1) in 40 m water, was visited about 1 hour before sunrise on 18, 21, 25 and 28 February 2002. Samples were taken with a rosette sampler equipped with twelve 10–liter PVC Niskin bottles with stainless-steel internal springs. Salinity and temperature were recorded with a SBE 9/11 conductivity-temperature-depth probe attached to the rosette sampler. Conductivity measurements were converted into practical salinity scale values with the equation of UNESCO (1985). Water samples for the analyses of dissolved oxygen, nutrient salts, dissolved and suspended organic carbon, nitrogen, phosphorus and carbohydrates, pigments and plankton counts were collected from five depths: the surface (50% Photosynthesis Available Radiation, PAR; 1.9 ± 0.4 m), the depth of the 25% PAR (10 ± 1 m), the depth of the 1% PAR (18 ± 1 m), 28 ± 2 m and the bottom (41 ± 2 m). Production/

respiration rates, estimated by the oxygen incubation method, were performed at the five levels too. Microzooplankton grazing experiments were performed only at the surface (50% PAR).

b. Wind and current measurements

Shelf winds were measured by the meteorological buoy of Puertos del Estado off Cabo Silleiro placed at 42.10N, 9.39W (Fig. 1). An Aanderaa DCM12 Doppler Current Meter was deployed on the seabed of the sampling site at 40 m depth for 24 days, recording current velocity and direction at 30 minutes intervals. Five overlapped layers of 11 m depth were measured, centerd at 6.5, 13.0, 19.5, 26.0 and 32.5 m approximately. Both subinertial winds and residual currents (subtidal variability) were calculated by means of an $A_{24}{}^2A_{25}$ filter (Godin, 1972) with a cut off period of 30 hours, passed to the time series to remove variability at tidal or higher frequencies.

c. Dissolved oxygen (O_2)

Samples were directly collected into calibrated 110 mL glass flasks and, after fixation with Cl_2Mn and NaOH/NaI, they were kept in the dark until analysis in the laboratory 24 h later. O_2 was determined by Winkler potentiometric end-point titration using a Titrino 720 analyser (Metrohm) with a precision of ± 0.5 μmol kg^{-1}.

d. Nutrient salts (NH_4^+, NO_2^-, NO_3^-, HPO_4^{2-}, H_4SiO_4)

Samples for nutrient analysis were collected in 50-mL polyethylene bottles; they were kept cold (4°C) until analysis in the laboratory using standard segmented flow analysis (SFA) procedures within 2 hours of their collection. The precisions were ± 0.02 μM for nitrite, ± 0.1 μM for nitrate, ± 0.05 μM for ammonium, ± 0.02 μM for phosphate and ± 0.05 μM for silicate.

e. Dissolved organic carbon (DOC) and nitrogen (DON)

Samples for dissolved organic matter (DOM) were collected into 500 mL acid–cleaned flasks and filtered through precombusted (450°C, 4 h) 47 mm ø Whatman GF/F filters in an acid-cleaned glass filtration system, under low N_2 flow pressure. Aliquots for the analysis of DOC/DON were collected into 10 mL precombusted (450°C, 12 h) glass ampoules. After acidification with H_3PO_4 to pH$<$ 2, the ampoules were heat-sealed and stored in the dark at 4°C until analysis. DOC and DON were measured simultaneously with a nitrogen-specific Antek 7020 nitric oxide chemiluminescence detector coupled in series with the carbon-specific Infra-red Gas Analyzer of a Shimadzu TOC–5000 organic carbon analyzer, as described in Álvarez-Salgado and Miller (1998). The system was standardized daily with a mixture of potassium hydrogen phthalate and glycine. The concentrations of DOC and total dissolved nitrogen (TDN) were determined by subtracting the average peak area from the instrument blank area and dividing by the slope of the standard curve. The

precision of measurements was ±0.7 μmol C L^{-1} for carbon and ±0.2 μmol N L^{-1} for nitrogen. Their respective accuracies were tested daily with the TOC/TDN reference materials provided by D. Hansell (Univ. of Miami). We obtained an average concentration of 45.7 ± 1.6 μmol C L^{-1} and 21.3 ± 0.7 μmol N L^{-1} (n = 26) for the deep ocean reference (Sargasso Sea deep water, 2600 m) minus blank reference materials. The nominal value for TOC provided by the reference laboratory is 44.0 ± 1.5 μmol C L^{-1}; a consensus TDN value has not been supplied yet, but a mean ± SD value of 22.1 ± 0.8 μmol N L^{-1} for four HTCO systems and 21.4 μmol N L^{-1} for one per sulphate oxidation method has been provided by Sharp *et al.* (2004) as a result of the Lewes intercalibration exercise. DON was obtained by subtracting TIN (=ammonium + nitrite + nitrate) to TDN.

f. Dissolved organic phosphorus (DOP)

Samples were collected and filtered as indicated for the DOC/DON samples. The filtrate was collected into 50 mL polyethylene containers and frozen at –20°C until analysis. It was measured by means of the SFA system for phosphate, after oxidation with $Na_2S_2O_8$/borax and UV radiation (Armstrong *et al.,* 1966). Only the organic mono-phosphoric esters are analysed because poly-phosphates are resistant to this oxidation procedure. Daily calibrations with phosphate, phenyl phosphate and adenosine 5′–monophosphate (AMP) in seawater were carried out. Standards of AMP were analysed in order to calculate the mono–phosphoric esters recovery (~80%). The precision of the method was estimated as ±0.04 μmol P L^{-1}.

g. Dissolved mono– and polysaccharides (MCHO and PCHO)

Sampling and storage procedures were identical to those for DOP samples. MCHO and PCHO were determined by the oxidation of the free reduced sugars with 2,4,6-tripyridyl-s-triazine (TPTZ) followed by spectrophotometric detection at 595 nm (Myklestad *et al.,* 1997). Quantification of MCHO and total dissolved carbohydrates (d–CHO) was made by subtracting the average peak height from the blank height, and dividing by the slope of the standard curve (glucose). The estimated accuracy was ±0.6 μmol C L^{-1} for MCHO and ±0.7 μmol C L^{-1} for d–CHO, and the detection limit was ~2 μmol C L^{-1}. See Nieto-Cid *et al.* (2004) for further details.

h. Particulate organic carbon and nitrogen (POC and PON)

Suspended organic matter was collected under low-vacuum on precombusted (450°C, 4 h) 25-mm ø Whatman GF/F filters (POC/PON, 500 mL of seawater). All filters were dried overnight and frozen (–20°C) before analysis. Measurements of POC and PON were carried out with a Perkin Elmer 2400 CHN analyzer. Filters were packed into 30 mm tin disks and injected in the vertical quartz furnace of the analyser where combustion to CO_2, N_2 and H_2O was performed at 900°C. After separation of the gas products into a chromatographic column, a conductivity detector quantified the C, N and H content of the

sample. Daily standards of acetanilide were analysed. The precision of the method was ± 0.3 μmol C L^{-1} and ± 0.1 μmol N L^{-1}.

i. Particulate organic phosphorus (POP)

The same procedures of collection and storage than for POC/PON were followed, after filtration of 250 mL seawater. It was determined by $H_2SO_4/HClO_4$ digestion at 220°C of the particulate material collected over Whatman GF/F filters. The phosphoric acid produced was analysed, after neutralisation, using the SFA procedure for phosphate. Standards of phosphate were run every day of analysis. The precision for the entire analysis was ± 0.02 μmol P L^{-1}.

j. Particulate carbohydrates (Cho)

About 250 mL of seawater were filtered and stored as indicated for POC, PON and POP. Cho determination was carried out by the anthrone method (Ríos *et al.,* 1998). It is based oin the quantitative reaction of sugars with anthrone in a strongly acid medium at 90°C to give an intensely colored compound. The absorption was measured at 625 nm. The method was calibrated daily with D-glucose standards. The estimated accuracy of the method was ± 0.1 μmol C L^{-1}

k. Chlorophyll (Chl)

One hundred mL of seawater was filtered through GF/F filters and frozen (–20°C) before analysis. Chl was determined with a Turner Designs 10000R fluorometer after 90% acetone extraction (Yentsch and Menzel, 1963). The estimated precision was ± 0.05 mg m^{-3}.

l. Pigment

Seawater samples (1.5 L) were fractionated by filtering onto a 47 mm diameter Millipore APFD filter (nominal pore size 2.7 μm) and the filtrate filtered again through a Millipore APFF filter (nominal pore size 0.7 μm). The filters were frozen at -80°C until analysis. Pigment analyses were performed as described by Zapata *et al.* (2000); frozen filters were extracted in 90% acetone and aliquots (140 μl) of clarified extracts were mixed with of MilliQ water (60 μl) immediately before injection in a Waters Alliance HPLC System (Milford, Massachusetts), comprising a separations module, a photodiode array detector and a fluorescence detector. The column (Symmetry C_8 column, 150 x 4.6 mm, 3.5 μm particle size) was themostatted at 25 °C. Mobile phases were: A = methanol : acetonitrile : aqueous pyridine solution (0.25 M pyridine, pH adjusted to 5.0 with acetic acid) in the proportions 50:25:25 (v/v/v), and B = acetonitrile : acetone (80:20 v/v). A segmented linear gradient was applied (time, % B): 0 min, 0 %; 18 min, 40 %; 22 min, 100 %; 38 min, 100 %. Flow rate was 1ml min^{-1}. Pigments were detected by their absorbance at 440 nm and in the case of chlorophylls by their fluorescence at 650 nm when excited at 440 nm.

Pigments were identified by co–chromatography with authentic standards and by diode array spectroscopy. HPLC calibration was performed using chlorophyll and carotenoid standards isolated from microalgal cultures (see Zapata *et al.,* 2000). The molar extinction coefficients provided by Jeffrey (1997) were used for pigment quantification.

m. Plankton counts

Plankton samples were preserved in Lugol's iodine and sedimented in composite sedimentation chambers. The sedimented volume (10–50 ml) depended on the chlorophyll concentration of the sample. The organisms were identified and counted to the species level, when possible, using an inverted microscope. Small species were counted along two transects at x250 and x400 magnification. The larger forms were counted from the whole slide at x100 magnification. Counts are representative for individuals > 5 μm.

n. Metabolic balance of the water column

Daily photosynthetic (Pg) and respiration (R) rates of the microplankton community were estimated by the oxygen light–dark bottle method (Strickland and Parsons, 1972). Samples collected before sunrise in 10 L Niskin bottles were transferred to black polyethylene carboys. Five levels were sampled: 50%, 25% and 1% of surface light, and two more depths below in the aphotic layer at 28 ± 2 m and 41 ± 2 m. The carboys were gently shaken before sampling to prevent sedimentation of the particulate material. Series of eleven 110 mL Winkler bottles composed of triplicate initial, and quadruplicate light and dark subsamples were filled. Each series of eleven bottles were incubated for 24 hours (starting within 1 hour of the sun rise) in incubators placed in the terrace of the base laboratory. The original temperature and light conditions at each sampling depth were reproduced in the incubators by mixing the appropriate proportions of the cold (10°C) and warm (30°C) water provided by the cultivation facility of the base laboratory and using increasing numbers of slides of a 1 mm mesh, respectively. Dissolved oxygen was determined by Winkler potentiometric end-point titration as indicated above.

o. Microzooplankton herbivory

Two experiments on 21 and 28 February 2002 were carried out with surface water using the modified dilution technique originally described by Landry and Hassett (1982). All experimental containers, bottles, filters and tubing were soaked in 10% HCl and rinsed with Milli Q water before each experiment. Water was collected just before the CTD cast with a 30 L Niskin bottle dipped twice. Water from the first dip was gravity filtered through a 0.2 μm Gelman Suporcap filter and combined with unfiltered seawater from the second dip in twelve 2.3 L clear polycarbonate bottles to obtain duplicates of 10, 20, 40, 60, 80 and 100% of plankton ambient levels. Bottles were completely filled and incubated for 24 hours at the original light (50% PAR) and temperature conditions in an incubator placed in the terrace of the base laboratory. Initial and final replicate subsamples of 250 ml were taken from all experimental bottles for the determination of chlorophyll concentration.

Table 1. Chemical composition of the main organic products of synthesis and early degradation of marine phytoplankton according to Fraga *et al.* (1998). Percentages (in weight) of each group correspond to the average composition of marine phytoplankton.

	Chemical formula	% (w/w)
Phosphorus compounds	$C_{45}H_{76}O_{31}N_{12}P_5$	12.0
Proteins	$C_{139}H_{217}O_{45}N_{39}S$	45.1
Chlorophylls a, b, c_1 and c_2	$C_{46}H_{52}O_5N_4Mg$	2.0
Lipids	$C_{53}H_{89}O_6$	16.5
Carbohydrates	$C_6H_{10}O_5$	24.4
Average composition	$C_{106}H_{171}O_{44}N_{16}P$	100.0

Chlorophyll samples were filtered onto 25 mm GF/F filters and extracted with 90% acetone for 24 h at –20°C. Chlorophyll concentration was determined by fluorometry using a Turner Designs fluorometer. Changes in the chlorophyll concentration were used to estimate the net growth rate ($\mu' = \mu - g$) of phytoplankton according to the equation:

$$\frac{1}{t} \cdot \ln\left(\frac{C_t}{C_0}\right) = \mu - g \cdot D \tag{1}$$

where t is the duration of the experiment (24 h), C_0 and C_t are the initial and final chlorophyll concentrations, respectively; μ and g are the instantaneous rates of phytoplankton growth and grazing mortality, respectively; and D is the dilution factor of the sample, which corresponds to the relative concentration of the prey and predator population. μ and g were estimated by linear regression of the daily net growth rate of phytoplankton (μ') against the dilution factor D.

p. Estimation of the chemical composition of biogenic materials

Fraga *et al.* (1998) reviewed in great detail the average composition of plankton carbohydrates (Cho), lipids (Lip), proteins (Prt), photosynthetic pigments (Chl) and phosphorus compounds (Pho), which is summarized in Table 1. This table also contains the relative contribution of each group to the average composition of marine phytoplankton. From the average composition of the biomolecules, the following set of five linear equations can be written for the suspended organic material:

$$C = 139 \times Prt + 6 \times Cho + 53 \times Lip + 45 \times Pho + 46 \times Chl \tag{2}$$

$$H = 217 \times Prt + 10 \times Cho + 89 \times Lip + 76 \times Pho + 52 \times Chl \tag{3}$$

$$O = 45 \times Prt + 5 \times Cho + 6 \times Lip + 31 \times Pho + 5 \times Chl \tag{4}$$

$$N = 39 \times Prt + 12 \times Pho + 4 \times Chl \tag{5}$$

$$P = 5 \times Pho \tag{6}$$

Since suspended C, N, P, Cho and Chl have been measured, the system can be solved to obtain the average chemical formula and the proportions of the different biomolecules for each particular sample. Once the biochemical composition of each sample is known, oxygen production rates (Pg, in m mol O_2 m^{-3} d^{-1}) can be converted into chlorophyll production rates (in mg Chl m^{-3} d^{-1}) using the resultant $R_C = \Delta O_2/\Delta C$org stoichiometric ratio and the Chl contribution to the suspended organic carbon pool.

3. Results

a. Water transports

Persistent north westerly winds of about -6 m s^{-1} blew on the shelf from 18 to 24 February and, then, they suddenly reversed to south easterlies producing a peak of 6 m s^{-1} on 27 February 2002 (Fig. 2a,b,c). This wind regime produced a 2-layered positive residual circulation pattern with an ingoing bottom current and an outgoing surface current from 18 to 24 February and a reversal of the flow from 24 to 28 February 2002 (Fig. 2d). The circulation pattern had a strong impact on the salinity (Fig. 2e) and temperature (Fig. 2f) distributions, characterized by the entry of cold (<13.5 °C) and salty (>35.8) Eastern North Atlantic Central Water (ENACW) through the bottom layer from 18 to 24 February, which is replaced by the colder (<13.2°C) and fresher (<35.4) shelf surface water through the surface from 24 to 28 February 2002. The impact of shelf winds on the thermohaline properties was substantially more decisive than continental inputs (Fig. 2b), quite reduced for this time of the year (Nogueira et al., 1997), or heat exchange across the sea surface (Fig. 2c).

b. Biochemical composition of the materials produced during the bloom

Ambient dissolved oxygen (Fig. 2g), dissolved inorganic nitrogen (Fig. 2h) and silicate (Fig. 2i) concentrations clearly indicated the impact of the *S. costatum* bloom (Table 2) on the chemistry of the water column with surface levels of 293 μmol O_2 kg^{-1}, 0.4 μmol N kg^{-1} and 0.94 μmol Si kg^{-1}, respectively, during 25 February 2002 when typical ambient concentrations for this time of the year are <250 μmol O_2 kg^{-1}, >4 μmol N kg^{-1} and >5 μmol Si kg^{-1}, respectively. More than 93% of the ambient dissolved inorganic nitrogen concentration during the study period was in the form of nitrate. Concomitantly, fluorometric chlorophyll levels (Fig. 2j) increased from >3 mg m^{-3} on 21 February to >14 mg m^{-3} on 25 February, four days later. Surprisingly, on 28 February, three days later, surface levels reduced to 4 mg m^{-3} and maximum chlorophyll concentrations of >11 mg m^{-3} were found in the bottom layer.

Diatoms and flagellates other than dinoflagellates were the main components of the microplankton population, accounting for 62–97% and 3–36% of the total cell abundance respectively (Table 2). Dinoflagellates and ciliates represented only a minor fraction. Diatoms were dominated by the chain–forming species *S. costatum* that accounted for 85–97% of diatom abundance, and small flagellates were almost the exclusive component

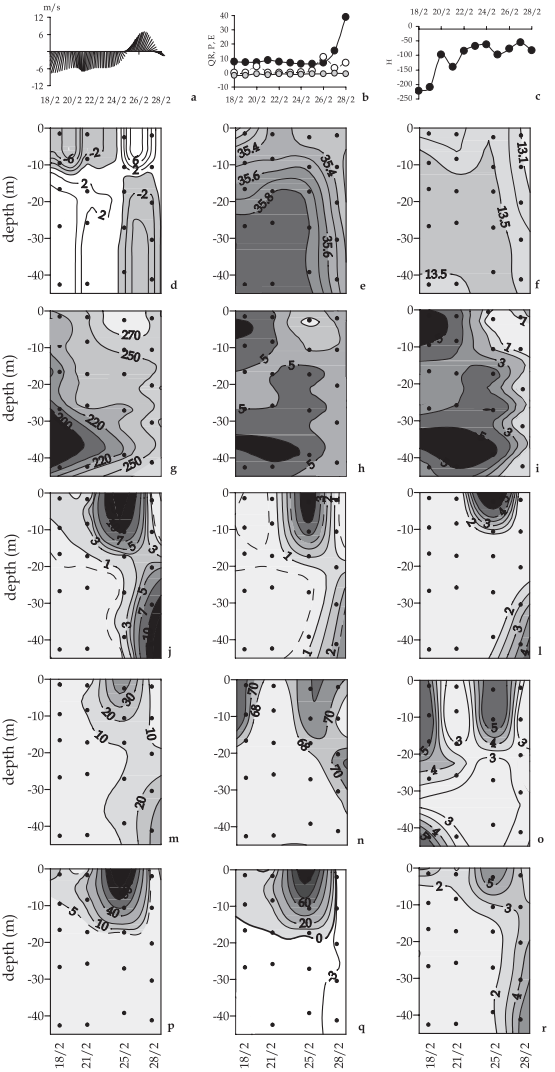

Figure 2. Time evolution of shelf winds, in m s^{-1} (a); continental runoff, precipitation and evaporation, in m^3 s^{-1} (b);, heat balance, in cal cm^{-2} d^{-1} (c); residual currents, in cm s^{-1} (d); salinity (e); temperature, in °C (f); dissolved oxygen, in μmol kg^{-1} (g), total inorganic nitrogen, in μmol kg^{-1} (h); silicate, in μmol kg^{-1} (i); Chlorophyll, in μg L^{-1} (j), fucoxanthin, in μg L^{-1} (k); suspended carbohydrates, in μmol L^{-1} (l); suspended organic carbon, in μmol L^{-1} (m); dissolved organic carbon , in μmol L^{-1} (n); dissolved carbohydrates, in μmol L^{-1} (o); gross primary production, in μmol kg^{-1} d^{-1} of O_2 (p); net primary production, μmol kg^{-1} d^{-1} of O_2 (q); and respiration, μmol kg^{-1} d^{-1} of O_2 (r). Panel b: black circles, continental runoff; grey circles, evaporation; open circles, precipitation.

Table 2. Mean ± SD cell abundance (cells mL^{-1}) of the main microplankton components (diatoms, dinoflagellates, other flagellates and ciliates) and the dominant species or group of species within each component. In brackets are the contribution of each component to the total microplankton abundance and the contribution of each species/group of species to the component abundance.

	18/02/02	21/02/02	25/02/02	28/02/02
Components				
Diatoms	191 ± 188 (70%)	348 ± 215 (62%)	16598 ± 14807 (97%)	797 ± 851 (72%)
Dinoflagellates	10 ± 4 (4%)	12 ± 3 (2%)	32 ± 22 (0.2%)	31 ± 18 (3%)
Other flagellates	72 ± 23 (26%)	205 ± 106 (36%)	469 ± 294 (3%)	282 ± 121 (25%)
Ciliates	1 ± 1 (0.3%)	1 ± 1 (0.2%)	2 ± 3 (0.01%)	3 ± 1 (0.3%)
Species/groups				
Skeletonema costatum	176 ± 182 (91%)	321 ± 200 (92%)	16029 ± 14404 (97%)	674 ± 876 (85%)
Small *Gymnodinium* spp.	5 ± 2 (45%)	5 ± 4 (42%)	15 ± 25 (49%)	20 ± 13 (65%)
Small flagellates	68 ± 23 (94%)	193 ± 96 (94%)	432 ± 277 (92%)	266 ± 126 (94%)
Small oligotrichous ciliates	0.6 ± 0.6 (76%)	0.7 ± 0.7 (87%)	1.2 ± 2 (63%)	1.5 ± 0.1 (46%)

of other flagellates. Coinciding with the outgoing surface flow, total cell numbers doubled, from a mean abundance of 275 cells mL^{-1} on 18 February to 565 cells mL^{-1} on 21 February. This rate of increase, about twice for other flagellates (0.6 d^{-1}) than for diatoms (0.3 d^{-1}), changed dramatically between 21 and 25 February when total cell number increased by 30 times. During this period, when the residual circulation stopped, diatoms accumulated at a rate of 11.7 d^{-1} (net doubling rate of 1.4 d^{-1}) considerably higher than for the other 3 groups (0.36 ± 0.06 d^{-1}). During the reversal of the residual circulation between 25 and 28 February, the microplankton population of the upper layer decreased at a rate of –0.31 d^{-1}, being –0.32 d^{-1} for diatoms and only -0.13 d^{-1} for other flagellates. The vertical distribution of diatoms in the photic layer was characterized by higher abundance at the surface than in the bottom of the photic layer on days 18, 21 and 25, whereas they were concentrated at 20 m (1% of incident light) on 28 February, where their abundance was 6 times higher than in shallower depths.

The results on pigment composition during the sampling period confirmed the predominance of diatom type pigments in the micro-and nanoplankton fraction (operationally defined as organisms retained in the 2.7 μm nominal pore size glass fibber filter, according to Rodríguez *et al.,* 2003). Pigments in this fraction are characterized by high contents of fucoxanthin (up to 3.77 μg L^{-1} in surface sample on 25 February) and chlorophyll c_2 (1.68 μg L^{-1} in the same sample) together with chlorophyll *a*. Only surface samples taken on 25 February traced amounts of chlorophyll c_3 and 19′–hexanoyloxyfucoxanthin that indicate the presence of flagellates belonging to the Division Haptophyta. Very small quantities of chlorophyll *b* (ranging from 0.01 to 0.04 μg L^{-1}) were detected on 25 and, specially, on 28 February, suggesting that the decay of the diatom bloom was followed by an increase in organisms representative of the Division Chlorophyta (as reflected in the changes of proportions of diatoms and flagellates that sampling day, see Table 2). In the fraction operationally corresponding to picoplankton (organisms passing through 2.7 but

retained by 0.7 μm nominal pore size glass fibber filter; Rodríguez *et al.,* 2003), only very small amounts of chlorophylls *b* and *a* were detected, indicating low photosynthetic biomass. The occurrence of chlorophyll *b* suggests the presence of cyanobacteria or, most probably and in agreement with cell counts ("small flagellates" in Table 2), small sized prasinophytes. This group was found to be abundant in this fraction in late winter samples in the neighbour Ría de Pontevedra (Rodríguez *et al.,* 2003).

The vertical distribution of pigments followed the developing and decay of the bloom, with chlorophyll c_2, and specially fucoxanthin (Fig. 2k), acting as good markers and paralleling the distribution of chlorophyll *a*. This fact supports the consideration that during the whole episode the main part of chlorophyll *a* was contributed by the same organism. During the onset of the bloom, fucoxanthin amounts began to be important in surface samples on 21 February (0.45 and 0.42 μg L^{-1} for the two upper samples, respectively). The development of the bloom (25 February) was characterized by very high amounts of fucoxanthin near the surface, which decreased dramatically in samples corresponding to 1 % PAR and lower. The decay of the bloom reversed the situation, with the highest values of fucoxanthin measured at the lower depths sampled on 28 February. It should be noted that during the decay of the bloom, average concentrations of each pigment in the water column did not suffer but slight variations (fucoxanthin changed from 1.54 μg L^{-1} on 25 February to 1.45 μg L^{-1} on 28 February, chlorophyll c_2 from 0.59 to 0.48 μg L^{-1} and chlorophyll *a* from 2.22 to 2.19 μg L^{-1}). The smaller variation in the average concentration of chlorophyll *a* is explained by the contribution of chlorophyll *a* from the Chlorophytes responsible for the presence of chlorophyll *b* on 28 February. Pigment/chlorophyll *a* ratios measured in the upper layer samples were the same as those measured in the lower layer samples during the decay of the bloom. For the case of the fucoxanthin/chlorophyll a ratio, it was 0.73, 0.68 and 0.65 at 50 % PAR, 25 % PAR and 1 % PAR on 25 February and 0.76, 0.68 and 0.65 at 1 % PAR, 28±2 m and 41±2 m, respectively, on 28 February.

The composition of the particulate organic material in the middle segment of the ría, calculated with Eqs. 2 to 6, was characterized by a quasi-constant proportion of carbohydrates of about 11% (mol C/mol C) and variable proportions of the most labile N– and P– rich materials and the most refractory lipids: pigments, proteins and phosphorus compounds proportions ranged from >60% (mol C/mol C) in the surface samples to <40% (mol C/mol C) in the bottom samples (Fig. 3). It contrasted with the composition of the particulate organic matter of continental origin, with higher proportions of carbohydrates (about 20% mol C/mol C). $1/\eta$, the ratio of chlorophyll to dissolved oxygen production in the upper layer, was calculated from the chemical formula of particulate organic matter and the calculated amount of oxygen produced during the synthesis of this material. The ratio ranged from 3 to 9 m mol O_2 mg Chl^{-1} (Table 3). The most commonly used $\Delta O_2/\Delta Corg$ ratio, also varied within a narrow interval (1.42 to 1.43 mol O_2 mol C^{-1}), close to the Redfield value of 1.4 (Laws, 1991; Anderson, 1995; Fraga, 2001).

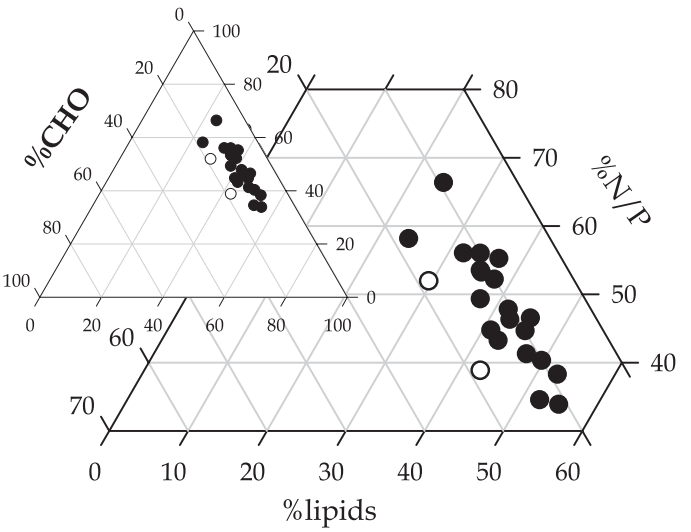

Figure 3. Ternary mixing diagram indicating the proportions of N and P compounds (chlorophyll + proteins + P compounds), carbohydrates and lipids in the particulate organic material of samples collected at stn 00. Solid dots, samples from stn 00; white dots, riverine samples.

c. Production and consumption rates of Chl a during the course of the bloom

The time evolution of Pg rates (Fig. 2p) is marked by the impressive surface maximum of more than 110 mmol O_2 m^{-3} d^{-1} on 25 February 2002, during the transition from northerly to southerly shelf winds, which led to an integrated primary production of 7.77 g C m^{-2} d^{-1} (Table 4). Since only 7.0% of the produced material was respired, 4.6% in the upper layer and 2.4% in the lower layer (Fig. 2r), most of it (Pn = 7.26 g C m^{-2} d^{-1}) was available for transference to higher trophic levels (grazing) and/or horizontal or vertical export (Fig. 2q; Table 4). On the contrary, three days later, after a brief downwelling episode (Fig, 2a,d,e & f), Pg rates had decreased to <20 m mol O_2 m^{-3} d^{-1} and R rates kept relatively high, specially at the bottom layer: 68.4 % of the produced material was respired

Table 3. Average composition of the biogenic materials in the upper and lower layer of the middle segment of the Ría de Vigo during the sampling period in February 2002. The stoichiometric ratio of conversion of O_2 changes into organic carbon changes, organic carbon changes into chlorophyll changes and O_2 changes into chlorophyll changes are provided.

Date	Chemical formula	$R_C = \frac{\Delta O_2}{\Delta Corg}$ (mol O_2 mol C^{-1})	$\frac{\Delta Corg}{\Delta Chl}$ (mmol C mg Chl^{-1})	$\frac{1}{\eta} = \frac{\Delta O_2}{\Delta Chl}$ (mmol O_2 mg Chl^{-1})
18/02/02	$C_{95}H_{154}O_{30}N_{12}P$	1.425	6.35	9.05
21/02/02	$C_{64}H_{104}O_{22}N_9P$	1.421	3.96	5.63
25/02/02	$C_{82}H_{132}O_{30}N_{13}P$	1.429	2.32	3.32
28/02/02	$C_{82}H_{133}O_{28}N_{11}P$	1.426	2.87	4.09

Table 4. Depth average gross (Pg) and net (Pn) primary production and respiration (R) rates in O_2, carbon and chlorophyll units for the upper and lower layer of the middle segment of the Ría de Vigo during the sampling period in February 2002. The $\Delta O_2/\Delta Corg$ and $\Delta Corg/\Delta Chl$ factors of Table 3 have been used to transform Pg rates from O_2 to carbon and Chl units. A constant $(\Delta O_2/\Delta Corg) = 1$ mol O_2 (mol C)$^{-1}$ (equivalent to carbohydrate respiration) was used to transform R from O_2 to carbon units.

		18/02/02		21/02/02		25/02/02		28/02/02	
		Upper	Lower	Upper	Lower	Upper	Lower	Upper	Lower
Pg	$\frac{mmolO_2}{m^2\,d^{-1}}$	71	0	138	0	925	0	201	0
	$\frac{gC}{m^2\,d^{-1}}$	0.6	0.0	1.17	0.0	7.77	0.0	1.69	0.0
	$\frac{mg\ Chl}{m^2\,d^{-1}}$	8	0	25	0	279	0	49	0
Pn	$\frac{mmolO_2}{m^2\,d^{-1}}$	46	−34	115	−29	882	−22	141	−77
	$\frac{gC}{m^2\,d^{-1}}$	0.30	−0.40	0.89	−0.35	7.26	−0.26	0.97	−0.93
	$\frac{mg\ Chl}{m^2\,d^{-1}}$	8	0	25	0	279	0	49	0
R	$\frac{mmolO_2}{m^2\,d^{-1}}$	25	34	23	29	43	22	60	77
	$\frac{gC}{m^2\,d^{-1}}$	0.30	0.40	0.28	0.35	0.52	0.26	0.72	0.93
	$\frac{mg\ Chl}{m^2\,d^{-1}}$	0	0	0	0	0	0	0	0

in the water column, 30% in the upper layer and 38.4% in the lower layer (Table 4). This maximum of respiration at the bottom coincided with high chlorophyll levels (Fig. 2j).

In summary, 11.3% of Pg during the sampling period (18–28 February 2002) was respired in the upper layer, 12.1% was respired in the lower layer and 76.6% was available for *in situ* grazing and horizontal (advection) or vertical (advection, diffusion, sedimentation) export.

Contrasting results were obtained from the two dilution experiments conducted in the surface layer of the middle segment on 21 and 28 February to evaluate the microzooplankton grazing (Fig. 4). On 21 February, i.e. during the onset of the *S. costatum* bloom, the growth rate (average ± standard error) was 1.32 ± 0.03 d^{-1} and the grazing rate 0.29 ± 0.04 d^{-1}. On the contrary, on 28 February, i.e. during the abrupt decay of the bloom, both the growth and grazing rates had reduced to a half of the values on 21 February: 0.64 ±

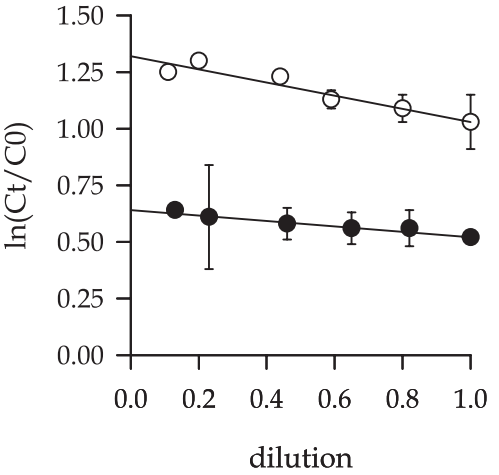

Figure 4. Results of the grazing incubation experiments conducted on 21 (open circles) and 28 (solid circles) February 2002 with water of 10 m depth at stn 00. The logarithm of the ratio between the final and initial Chlorophyll concentration is represented against the dilution factor to obtain the corresponding phytoplankton growth (intercept) and microzooplankton grazing (slope) rates.

0.01 and 0.12 ± 0.01 d^{-1}. Therefore, 20±3% of the daily primary production of the surface layer (50% PAR) was grazed by microheterotrophs. Assuming that this percentage is applicable to the whole study period and that the species composition of microheterotrophs and phytoplankton do not change with depth (Nogueira *et al.*, 2000), a constant with depth grazing rate was supposed. In addition, an average μ for the photic layer (μ_m) was calculated from the empirical μ at the 50% PAR and the proportion between the 50% PAR and the photic layer integrated O_2 primary production rate. The resultant μ_m was 0.69 d^{-1} on 21 February and 0.36 d^{-1} on 28 February. Then, the average Chl concentration in the photic layer (Chl_m) as a result of μ_m and g was calculated with the formula $Chl_m = Chl_0 (e^{(\mu-g)t} - 1)/(\mu-g)$ (Calvet and Landry, 2003). Finally, the photic layer integrated grazing rate, $G = g\ Chl_m$, was estimated; It was 12.1 mg Chl m^{-2} d^{-1} (48% of Pg) on 21 February and 11.5 mg Chl m^{-2} d^{-1} (23% of Pg) on 28 February, respectively. For the cases of 18 and 25 February, μ values were calculated on basis of the initial Chl concentration and the gross O_2 primary production at the 50% PAR. Values of 0.57 and 1.13 d^{-1} were obtained, respectively. The water column grazing rates (g), assumed to be 20% of the surface μ, was 0.11 and 0.23 d^{-1} on 18 and 25 February, respectively. Repeating the calculations performed for 21 and 28 February, it resulted that $\mu_m = 0.33\ d^{-1}$ and $G = 2.44$ mg Chl m^{-2} d^{-1} (20% of Pg) for 18 February and $\mu_m = 0.63\ d^{-1}$ and $G = 51.4$ mg Chl m^{-2} d^{-1} (23% of Pg) for 25 February.

4. Discussion

A time series study of coastal winds and surface chlorophyll levels revealed that winter upwelling events are relatively common in the rías of the NW Iberian Peninsula and they

used to be accompanied by remarkable chlorophyll peaks (Nogueira *et al.,* 1997). However, process-orientated studies of these winter upwelling events have not been conducted until recently (Álvarez-Salgado *et al.,* 2000; Pardo *et al*., 2001; Álvarez *et al.,* 2002) and they were focused on just the hydrographic and dynamic aspects. Until now, only a biogeochemical study of the net ecosystem production of dissolved organic carbon during a winter upwelling/downwelling sequence has been reported (Álvarez-Salgado *et al.,* 2001). Therefore, this is the first comprehensive study of the hydrodynamics and biogeochemistry of a winter phytoplankton bloom in the NW Iberian upwelling system. To our knowledge, there are no previous references to this phenomenon in other coastal upwelling systems at comparable latitudes (off Oregon and off Chile), where upwelling- and downwelling-favorable seasons can also be defined.

The average primary production of the Iberian shelf during the winter time is <0.5 g m^{-2} d^{-1} from satellite and *in situ* estimates (Joint *et al.*, 2002). During the course of the bloom, a rate as high as 7.8 gC m^{-2} d^{-1} was measured for an integrated Chl *a* concentration of 170 mg m^{-2} (surface Chl *a*, 14 mg m^{-3}) i.e. an assimilation number of 45 mg C (mg Chl)$^{-1}$. The assimilation number dramatically decreased to 2.3 mg C (mg Chl)$^{-1}$ during the decay of the bloom (28 February). While an assimilation number of 2.3 mg C (mg Chl)$^{-1}$ falls within the range of values obtained for the Ría de Vigo (Tilstone *et al.*, 1999) and for the adjacent shelf (Álvarez-Salgado *et al.*, 2003; Tilstone *et al.*, 2003) during spring and summer, 45 mg C (mg Chl)$^{-1}$ lies in the theoretical upper limit and, therefore, points to a high efficient phytoplankton carbon fixation. The resultant primary production rate was 3 times the average primary production of the productive upwelling season in the NW Iberian shelf: 2.5 g C m^{-2} d^{-1} (Arístegui *et al.*, 2005) or 2.1–2.7 g C m^{-2} d^{-1} in the middle Ría de Vigo (Moncoiffé *et al.*, 2000), a number which can be considered representative for coastal upwelling areas of the World Ocean (Wollast, 1998).

Average surface Chl *a* levels at the same site during the month of February from a time series of 9 years of measurements repeated twice a week ($n = 61$ data) was 2.7 mg m^{-3}, with 80% of the measurements within the 0–6 mg m^{-3} interval (Nogueira *et al.,* 1997). Therefore, surface Chl *a* levels on 25 February were five times the average and more than twice the 90% percentile. In fact, 14 mg m^{-3} represents the 90% percentile of Chl *a* concentration during the productive upwelling season, from May to October.

One of the possible fates of the produced material was respiration by the community of micro organisms that occupy the middle segment of the Ría de Vigo. In carbon units, microbial respiration was a relevant process before the onset (18 February) and during the decay of the bloom (28 February), when 50% and 43% of the produced carbon was respired in the photic layer, respectively. In fact, considering the respiration of the lower layer too, it resulted that the middle segment of the ría was close to balance ($Pg = R$) during those days. The high respiration rate recorded in the bottom layer during the decay of the bloom (0.9 g C m^{-2} d^{-1}) is especially remarkable. For comparison, during the upwelling season, Moncoiffé *et al.* (2000) obtained an average respiration of 0.5-0.6 g Cm^{-2} d^{-1} in the aphotic layer of the middle segment of the Ría de Vigo. In any case,

considering the study 10-d period, results show that 77% of the produced material was available for export to higher trophic levels, the adjacent shelf or the sediments. This ratio of exportable *versus* produced biogenic materials of 0.8, known as *f*- ratio after Eppley and Peterson (1979), is characteristic of the most productive marine ecosystems. For comparison, a mean *f*-ratio of 0.3 was obtained in the Ría de Vigo during the upwelling season of 1991 (Moncoiffé *et al.,* 2000) and 0.4 in the adjacent Ría de Arousa during the upwelling season of 1989 (Álvarez-Salgado *et al.,* 1996). The *f*–ratio of a coastal upwelling system rarely exceeds 0.5 (Wollast, 1998).

A second possible fate is grazing by microzooplankton. Although phytoplankton growth and grazing rates, estimated in this work from dilution experiments, fell in the range of values reported for other upwelling systems (Neuer and Cowles, 1994; Landry *et al.,* 1998; Edwards *et al.,* 1999), the relatively low grazing impact in the photic layer (21 ± 3% of phytoplankton growth, except on 18 February when it represented 48%) contrasted with that found by Fileman and Burkill (2001) in the shelf waters of the NW Iberian margin during summer, when microzooplankton herbivory was an important cause of phytoplankton mortality. This could be explained by the higher importance of microheterotrophs during summer (Figueiras and Ríos, 1993). In any case, microzooplankton herbivory did not play a relevant role in the decay of the study winter *S. costatum* bloom.

As a consequence of direct exudation and cell lysis during grazing processes, part of the produced material is released to the photic layer in the form of dissolved organic matter. During the development of the bloom, from 21 to 25 February, the DOC concentration in the photic layer increased from 65.0±0.5 to 70.8±0.5 m mol m^{-3}, i.e. at 1.5±0.7 m mol m^{-3} d^{-1} or 0.2 ± 0.1 g C m^{-2} d^{-1}. The average DOC excess of the surface compared with the bottom layer (ΔDOC), 2.1 ± 0.7 m mol m^{-3}, times the average surface outflow, 355 ± 188 m^3 s^{-1}, yields a net offshore DOC flux of 9 ± 4 g C s^{-1}. The surface outflow was calculated by multiplying the average surface velocity (Fig. 3c) times the corresponding cross section of the middle segment of the ría. Assuming that this flux is representative for a free surface area equivalent to the square of twice the internal Rossby radius of deformation, 1100 m (Cushman-Roisin, 1994), an extra DOC production of 0.16 ± 0.07 g C m^{-2} d^{-1} would be necessary to balance the offshore flux. Therefore, neglecting other transport processes, the net DOC production in the photic layer should be around 0.36±0.12 g C m^{-2} d^{-1} from February 21 to 25. This is <10% of the average Pg, as expected under mesotrophic conditions (Teira *et al.*, 2001a,b). In addition, <30% of ΔDOC was carbohydrates, a pattern that is also characteristic of nutrient-replete conditions (Normann *et al.*, 1995). By contrast, during the decay of the bloom, the DOC concentration in the photic layer decreased from 70.8 ± 0.5 to 67.5 ± 0.5 m mol m^{-3}, i.e. at –1.1 ± 0.7 m mol m^{-3} d^{-1} or –0.2±0.1 g C m^{-2} d^{-1}. This situation is typical of nutrient-deplete conditions, with microheterotrophs taking advantage of the situation. Net consumption of dissolved organic matter under downwelling conditions has been previously described in the Iberian upwelling system by Álvarez–Salgado *et al*. (2001). The absence of nutrients

produced that >70% of the DOC decrease in the surface layer were dissolved carbohydrates, a situation also typical of oligotrophic conditions (Normann *et al.,* 1995).

A fourth possible fate is the downward transport to the aphotic layer and the sediments. Considering the average Chl concentration of the photic layer (7.20 ± 0.05 mg m^{-3}) and the downward convective velocity (10 ± 2 m d^{-1}) obtained from the time evolution of the depth of the 35.5 isohaline (between 25 and 28 February),the result is a downward transport of 72 ± 12 mg Chl m^{-2} d^{-1}. This is 26 ± 2% of the average phytoplankton production (164 mg Chl m^{-2} d^{-1}) plus Chl import from the outer ría (88 ± 15 mg Chl m^{-2} d^{-1}) plus Chl loss in the photic layer (23.6 ± 0.4 mg Chl m^{-2} d^{-1}) from 25 to 28 February. The Chl import was obtained multiplying the average Chl concentration of the photic layer times the average surface inflow, 688 ± 255 m^3s^{-1}, and dividing by a surface area equivalent to the square of twice the internal Rossby radius of deformation. The Chl loss was calculated by subtracting the average concentration on 28 February from the average concentration on 25 February. Microzooplankton grazing represented 35 ± 5 mg Chl m^{-2} d^{-1}, i.e. 13±2% of the total Chl change in the middle ría. Assuming again that the downward convective flux is representative for a surface area equivalent to the square of twice the internal Rossby radius of deformation, the results show that the surface inward flow was not significantly different from the vertical downward flow. Therefore, sedimentation would be 169 ± 20 mg Chl m^{-2} d^{-1}; this is 61 ± 5% of the downward transport of Chl, at an average sedimentation rate of 15±3 m d^{-1}. This rate is within the range of variability of phytoplankton living and dead cells found in the literature (Druon and Le Fèvre, 1999). In a mesocosm study simulating a diatom winter/spring bloom, Riebesell (1989) found that the sedimentation rate of *S. costatum* increased from <0.5 m d^{-1} during the onset to >4 m d^{-1} during the decay. By contrast, other diatoms present in the mesocosm of Riebesell (1989), such as *Thalassiosira* spp. and *Leptocylindrus minimus*, sank at rates always <2 m d^{-1}. In any case, maximum sinking rates of S. costatum in the laboratory are 1.4 m d^{-1} (Smayda and Boleyn, 1966) which suggests that the high sinking rates measured in the field resulted from the formation of aggregates that increase in abundance during the decay of blooms (Riebesell, 1989) under condition of high phytoplankton biomass and temperature increase (Thornton and Thake, 1998).

The success of a phytoplankton population depends on its ability to strike a favorable balance between rates of cell division, grazing losses and sinking (Pitcher *et al.,* 1989). Comparison of the relevance of physical *versus* biogeochemical processes for the rapid decay of the *S. costatum* bloom revealed that sinking was the main mechanism removing cells from the photic layer in the ría. However, this high sedimentation rate was accompanied by an abrupt transition from upwelling to downwelling conditions; whereas upwelling promotes nutrient salts from the lower to the upper layer, this key fertilization mechanism is depressed under downwelling conditions. Therefore, nutrients depleted ($NO_3^- < 0.4$ μM N) during the blockage of the residual circulation in the middle ría from 21 to 25 February were not replenished from 25 to 28 February. The physiological mechanisms responsible for the regulation of phytoplankton buoyancy seem to be

determined by ambient light intensity and nutrient regime (Bienfang, 1981; Johnson and Smith, 1986; Culver and Smith, 1989). Therefore, the absence of nutrients was the probable cause of the large sedimentation rates from 25 to 28 February as observed in other diatom blooms (Smayda, 1970; Richardson and Cullen, 1995; Waite *et al.,* 1992). The later authors found that threshold nitrate concentrations approximating K_S values signalled the initiation of increased sedimentation. For the case of *S. costatum*, the threshold ambient nitrate level was 1 μM. Consequently, there seems to be a physically mediated biogeochemical control of the decay of the study winter *S. costatum* bloom.

Winter blooms are very relevant for the metabolic balance of the ecosystem because they represent a huge entry of freshly produced biogenic materials to the pelagic and benthic communities of the ría during a time when the primary production is commonly at low rates. In the study case, 70% of the material produced during the 10 d period was transferred to the lower layer of the ría. Only 20% of this material was respired by the heterotrophic microbial community of the aphotic layer and the remaining 80% would eventually feed the benthic communities. It is important to note that the fate of the bloom would be completely different if the period of calm would be followed by a new upwelling event. In that particular case, most of the material produced in the middle ría would be exported to the adjacent shelf and, eventually, would feed the benthic communities there. Furthermore, no pigment degradation products, apart from small amounts of chlorophyllide *a*, were observed during the decay of the bloom. Pigment/chlorophyll *a* ratios were the same in the photic layer during the development of the bloom as in cells sunk to the lower layer during the decay, strongly supporting that chloroplasts still keep their organization at this stage. It suggests that *S. costatum* cells could be still viable and, thus, able to bloom again if an immediate strong upwelling event (able to promote the sunk cell to the photic layer) succeeded after 28 February.

The biochemical composition of the produced materials is an excellent indicator of its nutritional quality for the pelagic and benthic communities. N and P compounds are preferentially used by microheterotrophs as substrates for structural and reproductive purposes. The average proportion of N and P compounds produced in the upper layer was 52% during the 10-d study period; this is about the average composition of marine phytoplankton (Laws, 1991; Anderson, 1995; Fraga, 2001). This proportion reduced to 47% in the aphotic layer, where the most refractory photosynthates, lipids, represented as much as 46%. This is the result of the preferential consumption of N and P compounds by the water column heterotrophs of the aphotic layer. Moreover, the material that arrived to the pelagic sediments is still of high quality, with proteins and phosphorus compounds representing 44% of the carbon deposited.

5. Conclusions

The extremely variable hydrographic conditions of the western coast of the Iberian Peninsula, characterized by a succession of shelf wind stress/relaxation events, allow the unusual development of massive phytoplankton blooms during the winter time. In 10 d, the

onset, development and decay of pioneer diatoms can occur, if the appropriate combination of upwelling (onset), relaxation (development) and downwelling (decay) conditions succeed. The downward transport of these winter blooms constitute the main entry of fresh materials to the benthic communities during the winter time.

Acknowledgments. The authors wish to thank the members of the Oceanography Group at the Instituto de Investigacións Mariñas (CSIC) and the Physical Oceanography Group at the University of Vigo who participated in this cruise. This work would not be possible without the cooperation of the captain, crew and technicians of R/V *Mytilus*. Financial support for this work came from the Spanish 'Ministerio de Educación y Ciencia' (MEyC), grant no. REN2000–0880–C02–01 MAR and the 'Xunta de Galicia' grant no. PGIDT01MAR40201PN. This is contribution no. 27 of the Unidad Asociada GOFUVI–CSIC. M.N.–C. and S. P. were funded by predoctoral fellowships of the Spanish Ministerio de Educación y Ciencia, B. G. C. was funded by a predoctoral fellowship of the CSIC–European Social Foundation I3P programme and I. C. G. T. was funded by a predoctoral fellowship of the Portuguese Fundação para a Ciência e a Tecnología.

References

Álvarez, I., M. deCastro, R. Prego, R. and M. Gomez-Gesteira. 2003. Hydrographic characterization of a winter–upwelling event in the Ria of Pontevedra (NW Spain). Estuar. Coast. Shelf Sci., 56, 869-876.

Álvarez–Salgado, X. A., S. Beloso, I. Joint, E. Nogueira, L. Chou, F. F. Pérez, S. Groom, J. M. Cabanas, A. P. Rees and M. Elskens. 2002. New production of the NW Iberian Shelf during the upwelling season over the period 1982–1999. Deep-Sea Res. I, *49*, 1725-1739.

Álvarez–Salgado, X. A., F. G. Figueiras, F. F. Pérez, S. Groom, E. Nogueira, A. V. Borges, L. Chou, C. G. Castro, G. Moncoiffé, A.F. Ríos, A. E. J. Miller, M. Frankignoulle, G. Savidge and R. Wollast. 2003. The Portugal Coastal Counter Current off NW Spain: New insights on its biogeochemical variability. Prog. Oceanogr., *56*, 281-321.

Álvarez–Salgado, X. A, J. Gago, B. M. Míguez, M. Gilcoto and F. F. Pérez. 2000. Surface waters of the NW Iberian margin: upwelling on the shelf *versus* outwelling of upwelled waters from the Rías Baixas. Estuar. Coast. Shelf. Sci., *51*, 821-837.

Álvarez–Salgado, X. A., J. Gago, B. M. Míguez and F. F. Pérez. 2001. Net ecosystem production of dissolved organic carbon in a coastal upwelling system: The Ría de Vigo, Iberian margin of the North Atlantic. Limnol. Oceanogr., *46*, 135-147.

Álvarez–Salgado, X. A. and A. E. J. Miller. 1998. Simultaneous determination of dissolved organic carbon and total dissolved nitrogen in seawater by high temperature catalytic oxidation: conditions for precise shipboard measurements. Mar. Chem., *62*, 325-333.

Álvarez–Salgado, X. A., G. Rosón, F. F. Pérez, F. G. Figueiras and Y. Pazos. 1996. Nitrogen cycling in an estuarine upwelling system, the Ría de Arousa (NW Spain). I. Short-time-scale patterns of hydrodynamic and biogeochemical circulation. Mar. Ecol. Prog. Ser., *135*, 259-273.

Anderson, L. A. 1995. On the hydrogen and oxygen content of marine phytoplankton. Deep-Sea Res. I, *42*, 1675-1680.

Arístegui, J., X. A. Álvarez–Salgado, E. D. Barton, F. G. Figueiras, S. Hernández–León, C. Roy and A. M. P. Santos. 2005. Oceanography and fisheries of the Canary Current Iberian region of the Eastern North Atlantic, *in* The Sea, *14*, K. H. Brink and A. R. Robinson, eds., John Wiley & Sons, NY, (*in press*).

Armstrong, F. A. J., P. M. Williams and J. D. H. Strickland. 1966. Photo–oxidation of organic matter in sea water by ultraviolet radiation, analytical and other applications. Nature, *211*, 481-483.

Bienfang, P. K. 1981. Sinking rates of heterogeneous, temperate phytoplankton populations. J. Plank. Res., *3*, 235-253.

Blasco, D., M. Estrada and B. Jones. 1980. Relations between the phytoplankton distribution and composition and the hydrography in the upwelling region near Cabo Corbeiro. Deep-Sea Res., *27*, 799-821.

Brink, K. H., B. H. Jones, J. C. Van Leer, C. N. K. Mooers, D. W. Stuart, M. R. Stevenson, R.C. Dugdale and G. W. Heburn. 1980. Physical and biological structure and variability in an upwelling center off Peru near 15S during March 1977, *in* Coastal Upwelling, F.A. Richards, ed., Am. Geophys. Union, Washington DC, 473-495.

Calvert, A. and M. R. Landry. 2003. Phytoplankton growth, microzoplankton grazing and carbon cycling in marine systems. Limnol. Oceanogr., *49,* 51–57.

Cushman-Roisin, B. 1994. Introduction to Geophysical Fluid Dynamics, Prentice Hall, Englewood Cliffs, NJ, 320 pp.

Culver, M. E. and W. O. Smith Jr. 1989. Effects of environmental variation of sinking rates of marine phytoplankton. J. Phycol., *25*, 262-270.

Druon, J. N. and J. Le Fèvre. 1999. Sensitivity of a pelagic ecosystem model to variations of process parameters within a realistic range. J. Mar. Syst., *19*, 1-26.

Edwards, E. S., P. H. Burkill and C. E. Stelfox. 1999. Zooplankton herbivory in the Arabian Sea during and after the SW Monsoon, 1994. Deep-Sea Res. II, *46*, 843-863.

Eppley, R. W. and B. J. Peterson. 1979. Particulate organic matter flux and planktonic new production in the deep ocean. Nature, *282*, 677-680.

Estrada, M. and D. Blasco. 1979. Two phases of the phytoplankton community in the Baja California upwelling. Limnol. Oceanogr., *24*, 1065-1080.

FAO Fisheries. 1997. Review of the state of World Fisheries Resources: Marine Fisheries Marine Resource Service. Fishery Resources Division, Fisheries Dept., Rome.

Fermín, E. G., F. G. Figueiras, B. Arbones and M. L. Villarino. 1996. Short time scale development of a *Gymnodinium catenatum* population in the Ría de Vigo (NW Spain). J. Phycol., *32*, 212-221.

Figueiras, F. G., K. J. Jones, A. M. Mosquera, X. A. Álvarez–Salgado, A. Edwards and N. MacDougall. 1994. Red tide assemblage formation in an estuarine upwelling ecosystem: Ría de Vigo. J. Plankton Res., *16*, 857-878.

Figueiras, F. G. and A. F. Ríos. 1993. Phytoplankton succession, red tides and the hydrographic regime in the Rias Bajas of Galicia, *in* Toxic Phytoplankton Blooms in the Sea, T. J. Smayda and Y. Shimizu, eds., Elsevier Science Publishers, 239-244.

Fileman, E. and P. Burkill. 2001. The herbivorous impact of microzooplankton during two short-term Lagrangian experiments off the NW coast of Galicia in summer 1998. Prog. Oceanogr., *51*, 361-383.

Fraga, F. 2001. Phytoplankton biomass synthesis: application to deviations from Redfield stoichiometry. Sci. Mar., *65*, 153-169.

Fraga, F., A. F. Ríos, F. F. Perez and F. Figueiras. 1998. Theoretical limits of oxygen: carbon and oxygen: nitrogen ratios during photosynthesis and mineralisation of organic matter in the sea. Sci. Mar., *62*, 161-168.

Godin, G. 1972. The Analysis of Tides, University of Toronto Press, 264 pp.

Jeffrey, S. W. 1997. Chlorophyll and carotenoid extinction coefficients, *in* Phytoplankton Pigments in Oceanography, S. W. Jeffrey, R. F. C. Mantoura and S.W. Wright, eds., Unesco Publishing, Paris, 595-596.

Johnson, T. O. and W. O. Smith. 1986. Sinking rates of phytoplankton assemblages in the Weddell Sea marginal ice zone. Mar. Ecol. Prog. Ser., 33, 131-137.

Joint, I., S. B. Groom, R. Wollast, L. Chou, G. H. Tilstone, F. G. Figueiras, M. Loijens and T. J. Smyth. 2002. The response of phytoplankton production to periodic upwelling and relaxation events at the Iberian shelf break: estimates by the 14C method and by satellite remote sensing. J. Mar. Syst., *32*, 219-238.

Landry, M. R., S. L. Brown, L. Campbell, J. Constantinou and H. Liu. 1998. Spatial patterns in phytoplankton growth and microzooplankton grazing in the Arabian Sea during monsoonal forcing. Deep-Sea Res. II, *45*, 2353-2368.

Landry, M. R. and R. P. Hasset. 1982. Estimating the grazing impact of marine micro-zooplankton. Mar. Biol., *67*, 283-288.

Laws, E. A. 1991. Photosynthetic quotients, new production and net community production in the open ocean, Deep-Sea Res., *38*, 143-167.

Margalef, R. 1978. Phytoplankton communities in upwelling areas. The example of NW Africa. Oecologia Aquatica, *3*, 97-132.

Middelburg, J. J., T. Vlug, F. Jaco and W. A. van der Nat. 1993. Organic matter mineralization in marine systems. Global Planet. Change, *8*, 47-58.

Moncoiffé, G., X. A. Álvarez–Salgado, F. G. Figueiras and G. Savidge. 2000. Seasonal and short time-scale dynamics of microplankton community production and respiration in an inshore upwelling system. Mar. Ecol. Prog. Ser., *196*, 111-126.

Myklestad, S. M., E. Skanoy and S. Hestmann. 1997. A sensitive and rapid method for analysis of dissolved mono– and polysaccharides in seawater. Mar. Chem., *56*, 279-286.

Neuer, S. and T. J. Cowles. 1994. Protist herbivory in the Oregon upwelling system. Mar. Ecol. Prog. Ser., *113*, 147–162.

Nieto-Cid, M., X. A. Álvarez–Salgado, S. Brea and F. F. Pérez. 2004. Cycling of dissolved and particulate carbohydrates in a coastal upwelling system (NW Iberian Peninsula) Mar. Ecol. Prog. Ser., *284*, 39-54. (is this correct)

Nogueira, E., F. Ibanez and F. G. Figueiras. 2000. Effect of meteorological and hydrographic disturbances on the microplankton community structure in the Ria de Vigo (NW Spain). Mar. Ecol. Prog. Ser., *203*, 23-45.

Nogueira, E., F. F. Pérez and A. F. Ríos. 1997. Seasonal patterns and long-term trends in an estuarine upwelling ecosystem (Ría de Vigo, NW Spain). Estuar. Coast. Shelf Sci., *44*, 285-300.

Normann, B., U. L. Zweifel, C. S. Hopkinson and B. Fry. 1995. Production and utilization of dissolved organic carbon during an experimental diatom bloom. Limnol. Oceanogr., *40*, 898-907.

Pardo, P. C., M. Gilcoto and F. F. Pérez. 2001. Short time-scale coupling between themohaline and meteorological forcing in the Ría de Pontevedra. Sci. Mar., *65 (Suppl. 1*), 229-240.

Pazos, Y., F. G. Figueiras, X. A. Álvarez-Salgado and G. Rosón. 1995. The control of succession in red tide species in the Ría de Arousa (NW Spain) by upwelling and stability, *in* Harmful Marine Algal Blooms, Lavosier, 645-650.

Pérez, F. F. and F. Fraga. 1987. A precise and rapid analytical procedure for alkalinity determinations. Mar. Chem., *21*, 169-182.

Pitcher, G. C., D. R. Walker and B. A. Mitchell-Innes. 1989. Phytoplankton sinking rate dynamics in the southern Benguela upwelling system. Mar. Ecol. Prog. Ser., *55*, 261-269.

Richardson, T. L. and J. J. Cullen. 1995. Changes in buoyancy and chemical composition during growth of a coastal marine diatom: ecological and biogeochemical consequences. Mar. Ecol. Prog. Ser., *128*, 77-99.

Riebesell, U. 1989. Comparison of sinking and sedimentation rate measurements in a diatom winter /spring bloom. Mar. Ecol. Prog. Ser., *54*, 109-119.

Ríos, A. F., F. Fraga, F. F. Pérez and F. G. Figueiras. 1998. Chemical composition of phytoplankton and particulate organic matter in Ría de Vigo (NW Spain). Sci. Mar., *62*, 257-271.

Rodríguez, F., Y. Pazos, J. Maneiro and M. Zapata. 2003. Temporal variation in phytoplankton assemblages and pigment composition at a fixed station of the Ría of Pontevedra (NW Spain). Estuar. Coast. Shelf Sci., *58*, 499-515.

Sharp, J. H., A. Y., Beauregard, D. Burdige, G. Cauwet, S. E. Curless, R. Lauck, K. Nagel, H. Ogawa, A. E. Parker, O. Primm, M. Pujo–Pay, W. B. Savidge, S. Seitzinger, G. Spyres and R.

Styles. 2004. A direct instrument comparison for measurement of total dissolved nitrogen in seawater. Mar. Chem., *84*, 181-193.

Smayda, T. J. 1970. The suspension and sinking of phytoplankton in the sea. Oceanogr. Mar. Biol. A. Rev., *8*, 353-414.

Smayda, T. J. and B. J. Boylen. 1966. Experimental observations on the flotation of marine diatoms. II. *Skeletonema costatum* and *Rhizosolenia setigera*. Limnol. Oceanogr., *11*, 18-34.

Strickland, J. D. and T. R. Parsons. 1972. A Practical Handbook of Seawater Analysis, 2nd ed., Bull. Fish. Res. Bd. Canada, 167 pp.

Teira, E., M. J. Pazó, P. Serret and E. Fernández. 2001a. Dissolved organic carbon production by microbial populations in the Atlantic Ocean. Limnol. Oceanog., *46***,** 1370-1377.

Teira, E., P. Serret and E. Fernández. 2001b. Phytoplankton size–structure, particulate and dissolved organic carbon production and oxygen fluxes through microbial communities in the NW Iberian coastal transition zone. Mar. Ecol. Prog. Ser., *219***,** 65-83.

Thornton, D. C. O. and B. Thake. 1998. Effect of temperature on the aggregation of *Skeletonema costatum* (Bacillariophyceae) and the implication fro carbon flux in coastal waters. Mar. Ecol. Prog. Ser., *174*, 223-231.

Tilstone, G. H., F. G. Figueiras, E. G. Fermín and B. Arbones. 1999. The significance of nano-phytoplankton photosynthesis and primary productivity in a coastal upwelling ecosystem (Ría de Vigo, NW Spain). Mar. Ecol. Prog. Ser., *205*, 23-41.

Tilstone, G. H., F. G. Figueiras, L. M. Lorenzo and B. Arbones. 2003. Phytoplankton composition, photosynthesis and primary production during different hydrographic conditions at the Northwest Iberian upwelling system. Mar. Ecol. Prog. Ser., *252*, 89-104.

UNESCO. 1985. The international system of units (SI) in oceanography. UNESCO Tech. Papers in Mar. Sci., 45, 1-124.

Waite, A., P. K. Bienfang and P. J. Harrison. 1992. Spring bloom sedimentation in a subartic ecosystem. II. Succession and sedimentation. Mar. Biol, *114*, 131-138.

Walsh, J. J. 1991. Importance of continental margins in the marine biogeochemical cycling of carbon and nitrogen. Nature, *359*, 53-55.

Wollast, R. 1998. Evaluation and comparison of the global carbon cycle in the coastal zone and in the open ocean, *in* The Sea, *10*, K. H. Brink and A. R. Robinson, eds., John Wiley & Sons, NY, 213-252.

_____1993. Interactions of carbon and nitrogen cycles in the coastal zone, *in* Interaction of C, N, P and S Biochemical Cycles and Global Change, R. Wollast, F. P. Mackenzie and L. Chou, eds., Springer-Verlag, Berlin, 195-210.

Yentsch, C. S. and D. W. Menzel. 1963. A method for the determination of phytoplankton chlorophyll and phaeophytin by fluorescence. Deep-Sea Res., *10*, 221-231.

Zapata, M., F. Rodríguez and J. L. Garrido. 2000. Separation of chlorophylls and carotenoids from marine phytoplankton: a new HPLC method using a reversed phase C8 column and pyridine–containing mobile phases. Mar. Ecol. Prog. Ser., *195*, 29–45.

Received: *22 July, 2004*; revised: *22 July, 2005*.